

Impedance Study of Spinel Type Fe-Co₃O₄ Oxide Thin Film Electrodes in Alkaline Medium

E. Laouini¹, M. Hamdani^{1*}, M.I.S. Pereira², Y. Berghoute¹, J. Douch¹, M. H. Mendonça², R.N. Singh³

¹ Laboratoire de Chimie Physique, Faculté des Sciences, Université Ibn Zohr, B.P. 8106 /S Cité Dakhla, Agadir Maroc.

* E-mail : hamdani.mohamed@gmail.com

² Centro de Ciências Moleculares e Materiais Faculdade de Ciências da Universidade de Lisboa Portugal.

³ Department of Chemistry, Faculty of Science, Banaras Hindu University, Varanasi 221 005, India.

Received: 29 May 2009 / Accepted: 12 August 2009 / Published: 25 August 2009

Spinel type Fe-Co₃O₄ (0, 5 and 10 % of Fe) oxide thin films have been investigated as electrocatalysts for the oxygen evolution reaction (OER) in 1M KOH using electrochemical impedance spectroscopy (EIS) technique. The oxide films were prepared, on stainless steel supports, using the thermal decomposition method at 400°C. The EIS study was carried out to investigate the effect of the partial substitution of Co by Fe, in the oxide lattice, on the catalytic performance towards the OER and also on the oxide film /1M KOH interface. The observed results have been compared with those reported in literature for similar oxide film electrodes, obtained by cyclic and steady-state voltammeteries under similar experimental conditions. The EIS measurements were fitted, using an electrical equivalent circuit L (R₁Q₁) (R₂Q₂), in the oxidative process, from 0 V to 0.700 V vs. SCE. At each potential, a good correlation between experimental and simulated data is found, validating thereby the proposed equivalent circuit model.

Keywords: Thin films, electrocatalysis, iron-cobalt oxide electrode, EIS, oxygen evolution

1. INTRODUCTION

Cobalt oxides with the spinel type structure are of interest as electrode materials due to their stability and electrocatalytic activity towards the oxygen evolution reaction (OER) [1-6]. Thus, the development of highly active, stable and low-cost electrocatalysts is a major issue. The high overpotential of OER is the main problem that postpones the use of low-cost anodes in water electrolysis cells. Efforts are made to improve the reaction kinetics and lower the overpotential.

In recent years, spinel-type transition metal oxides mainly cobalt oxide (Co₃O₄) are reported as promising anode materials for the OER in alkaline media [7-9]. Usually, these oxide catalyst coatings

are made by thermal deposition on suitable metallic substrate. However, Co_3O_4 has been prepared recently in different forms including nanoparticules [7], nanorods [8] and nanofibres [9] using cobalt organic precursors or cobalt nitrate in organic solvents. In spite of this, the electrocatalytic properties and stabilities of these nanostructured materials are not yet studied.

The electrochemical impedance spectroscopy (EIS) has recently received great attention, due to its ability to characterize the electrochemical and electrocatalytic interfacial surface properties of oxide electrodes towards the OER, as well as to understand solid state surface redox transitions (SSSRT). Indeed, the electrical circuit, represented by $R_s L(R1Q1) (R2Q2) (R3Q3)$ has been proposed, where (R1Q1), (R2Q2) and (R3Q3) correspond to the capacitive and resistive contributions of the barrier layer / metal interface, the bulk barrier layer and the electrolyte / barrier layer interface, respectively and L is an inductance [10-13]. Other electrical equivalent circuits that describe the oxide/1M KOH solution interface are also referred in literature [14-16]. However, for porous oxide catalyst electrodes the simpler and more frequently used electrical equivalent circuit to describe the characteristics of the interface has been the $R_s(R1Q1)(R2Q2)$ [14,17]. A similar model has also been proposed by Silva et al. [18] for cobalt oxide coatings on cold-rolled steel in alkaline sodium sulphate.

Very recently, we have prepared Fe- substituted Co_3O_4 films, on a stainless steel substrate, by thermal decomposition of nitrate precursors and investigated them in 1M KOH by EIS at several oxidative dc potentials, starting from the open circuit potential to the oxygen evolution potential. The objective of the study has been to obtain the OER kinetic parameters from impedance measurements and compare the values, so obtained, with those previously obtained from steady-state Tafel polarisation studies, on the same oxide electrodes [10]. The proposed equivalent circuit to fit the impedance results and describe the characteristics of the interface was the $R_s (R1Q1) (R2Q2)$. A similar model is also referred in the literature [14, 17, 18]. More recently one of us and his collaborators [19] have also employed similar equivalent circuit model to treat the impedance data obtained for Co_3O_4 and La-doped Co_3O_4 in 1 M KOH. The latter oxides were prepared by a microwave-assisted synthesis in the form of thin films on Ni.

2. EXPERIMENTAL PART

2.1. Oxide film electrodes preparation

The Fe- Co_3O_4 films (Fe/Co = 0, 5, 10 %) were prepared by thermal decomposition of mixed metal nitrates on stainless steel supports with dimensions, 1 cm \times 2 cm \times 0.1 cm following the procedure described previously [10, 11]. The pre-treated steel plates were placed in a drying oven at 60 °C and small drops of the mixed metal nitrates solution were then spread on one side of the surface using a syringe. After the solvent evaporation, small drops of the solution were dripped again on the surface and dried. The coating procedure was repeated 4 to 5 times to produce an uniform dehydrated salt on the support. The dried coatings were finally annealed at 400 °C for 2 h in a furnace to obtain adherent thin oxide black colored films. The oxide loadings ranged between 2.0 and 2.4 mg cm^{-2} (3 to 4 μm thick). The prepared films present a good adherence to the substrate.

A single electrode face was in contact with the electrolyte (2 cm^2). The opposite face was covered with an inactive and non-conductive varnish. The electrical contact with the oxide film was made as already described [10-11].

2.2. Electrochemical studies

The electrochemical impedance spectroscopy (EIS) study has been carried out in a conventional three-electrode single compartment glass cell (80 ml) using 1 M KOH as the electrolyte. The auxiliary and reference electrodes were a platinum plate of 8 cm^2 and a saturated calomel electrode (SCE) (0.240 V vs SHE), respectively. In order to minimize the solution resistance, the reference electrode was connected to the electrolyte through a Lugging capillary containing an aqueous agar-agar (KCl) salt bridge, placed as close as possible to the surface of the working electrode.

The EIS study was performed using a computerized potentiostat electrochemical set (Voltalab PRZ 100 Radiometer-Analytical). Zview software was used to analyze the data. The experimental impedance data were fitted to an appropriate equivalent circuit using ZsimpWin software. The experimental procedures and conditions employed in the EIS study were similar to those described previously [10-11]. Before starting the investigation, the electrolyte was invariably deaerated for 20 min using pure nitrogen flux and the open-circuit potential (OCP) was then measured. The electrodes reached stable OCP values, $0 \pm 5 \text{ mV vs. SCE}$, after 3 to 5 min of their dipping in the electrolyte, regardless of the composition. An AC voltage amplitude of 5 mV and a frequency range of 0.01-105 Hz were employed in the impedance measurements. Results are displayed in the form of Bode and Nyquist plots. All electrochemical experiments were carried out in deaerated 1 M KOH (Merck) at $25 \pm 1 \text{ }^\circ\text{C}$.

3. RESULTS AND DISCUSSION

Impedance spectra for the investigated oxides in 1M KOH were recorded at different potentials, between 0 and 0.800 V vs. SCE at $25 \text{ }^\circ\text{C}$. The potentials values were selected in order to observe the electrodes behavior, namely the pseudo capacitance ($E = 0.200 \text{ V}$, Fig 1), the $\text{Co}^{4+}/\text{Co}^{3+}$ redox couple transition ($E = 0.400$, Fig 2) and the oxygen evolution ($E = 0.500 \text{ V}$ and 0.600 V , Fig 3 and 4). As mentioned earlier [11], before each measurement, the electrode was allowed to equilibrate at each applied dc potential. Impedance data were displayed in the form of Nyquist and Bode plots (denoted (a) and (b) respectively on the figures).

As it can be seen, each complex-plane diagram (Nyquist) is characterized by three distinct regions, low, intermediate and high frequency regions. However, only at intermediate and high frequencies, the features of all the curves are similar, regardless of the applied dc potential. At high frequencies, the influence of inductance on impedance predominates and increases with the increasing frequency. Note that this inductance is not associated with the electrode process, but is a contribution from the cell connections and their interaction with the surroundings [20]. At intermediate frequencies, all the curves show the formation of a depressed semicircle.

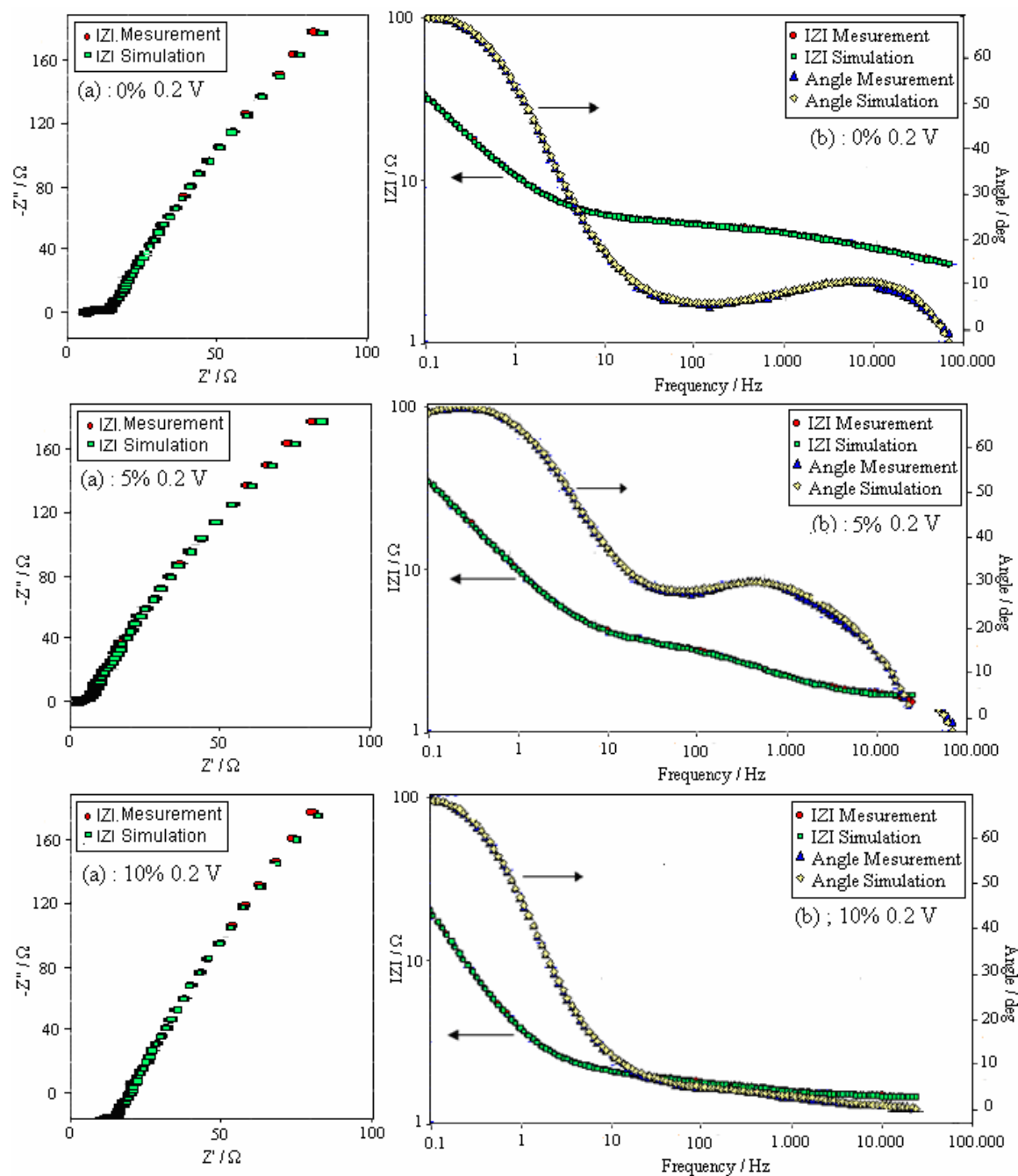


Figure 1. Complex impedance (a) Nyquist and (b) Bode plots, for Fe-Co₃O₄ in 1 M KOH, E = 0.200 V vs SCE. Experimental and simulated results.

At low frequencies, and for E = 0.200 V (prior to the O₂ evolution region), Figs. 1 (a) the sloping line on the Nyquist plots indicates that the Fe-Co₃O₄ / 1 M KOH interface exhibits a capacitive behaviour. This may be caused by the diffusion of the charged species (H⁺ / OH⁻), into the oxide film, through defects and pores [21, 22]. The capacitive behaviour of the electrode / electrolyte interface at low frequencies is common in cases of ions intercalation into inorganic / polymer matrix [23]. On the contrary, when E ≥ 0.5 V, in the O₂ evolution region, (Figs.3), the low frequency end of the Nyquist

plots show a semicircle, the diameter of which decreases with increasing E (or overpotential, η). Thus, the formation of a potential dependent semicircle at $E \geq 0.5$ V in the low frequency region can be ascribed to the OER. Fig. 4 shows a typical complex plane (experimental and simulated) for the pure oxide coating at 0.600 V vs SCE. The same trend was obtained for the two Fe containing oxides. The radius of the second semicircle, corresponding to OER, decreased as the overpotential increased. A similar diagram was already reported in the literature for Co_3O_4 electrode under oxygen evolution [18].

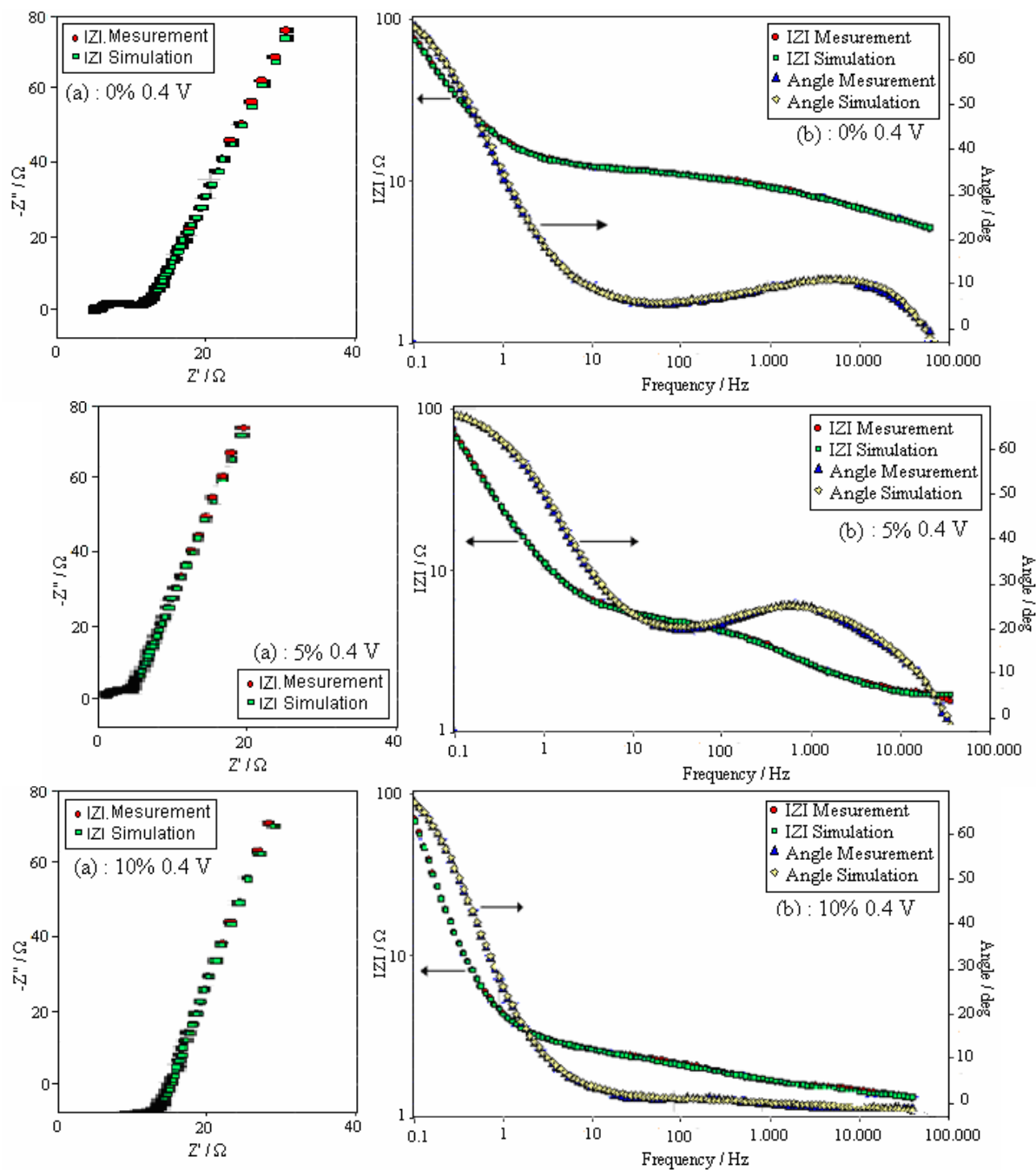


Figure 2. Complex impedance (a) Nyquist and (b) Bode plots, for Fe- Co_3O_4 in 1 M KOH, $E = 0.400$ V vs SCE. Experimental and simulated results.

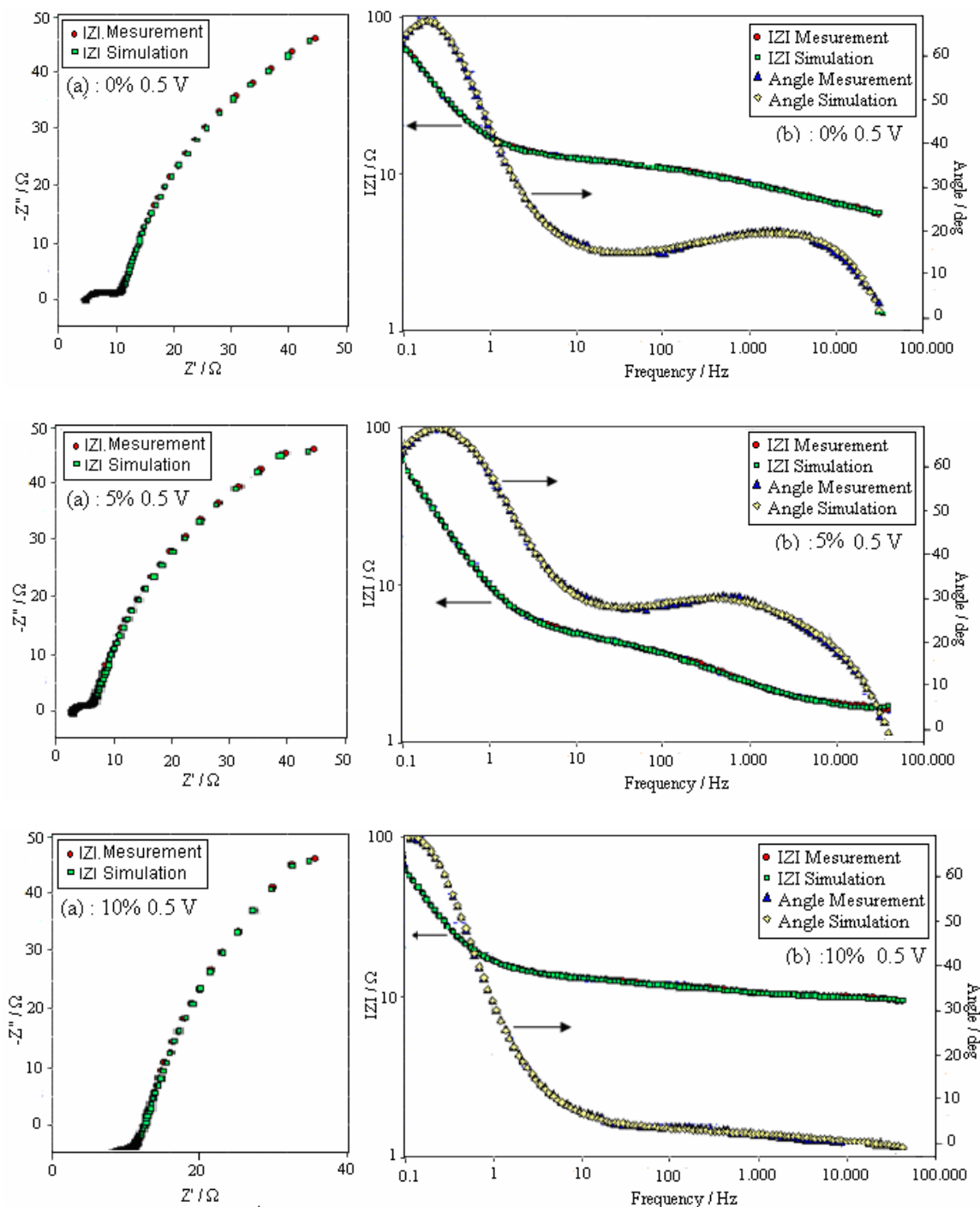


Figure 3. Complex impedance (a) Nyquist and (b) Bode plots, for Co_3O_4 in 1 M KOH, $E = 0.500$ V SCE. Experimental and simulated results.

The catalyst/ electrolyte interface description is given in terms of an equivalent circuit, composed of an inductive and two capacitive/resistive elements in series, of the form $\text{LRs}(\text{R}_1\text{Q}_1)(\text{R}_2\text{Q}_2)$ corresponding to a simple model employed for porous oxide electrodes [14,17,18]. The symbols, L, Rs, R1, R2, Q1, and Q2 represent inductance (H), solution resistance (Ω), oxide film

(bulk) resistance (Ω), charge transfer resistance (Ω), constant phase element ($Q1 = CPE$) corresponding to the oxide mass and CPE corresponding to the film/1 M KOH interface, respectively.

The simulated results are in good agreement with the experimental data. The resultant EIS parameters from this equivalent circuit used to simulate the impedance data are given in Tables 1-3 for 0, 5 and 10 % Fe. The fitting procedure showed that the best agreement between the experimental and simulated data was obtained when a constant phase element (CPC) was used instead of a pure capacitance.

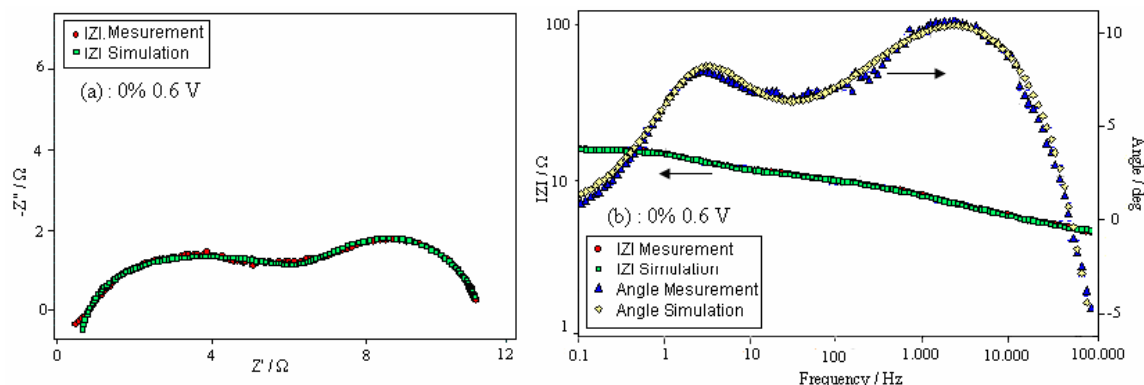


Figure 4. Complex impedance (a) Nyquist and (b) Bode plots, for Co_3O_4 0% in 1 M KOH, $E = 0.600$ V vs SCE. Experimental and simulated results.

The EI spectra obtained from the proposed circuit model, agree reasonably well with the experimental curves as shown in the Figs 1 to 4. Chi-square (χ^2) values of the order of 10^{-4} were obtained, which are quite reasonable for the validity of a model. Estimates of the circuit parameters of the electrical equivalent circuit are displayed in Tables 1-3. The time constants, τ_1 and τ_2 corresponding to each sub circuit, namely (R_1Q_1) and (R_2Q_2) have also been estimated at the different applied potentials using the relation,

$$\tau^n = R \cdot Q \quad (1)$$

and the values are also given in Tables 1-3.

It can be seen that τ_1 value for the resistive/ capacitive subcircuit (R_1Q_1) is the lowest and the R_1 and Q_1 values show a slight variation with potential. Therefore, (R_1Q_1) can be assigned to the properties of the bulk oxide; being R_1 the resistance of the oxide film. The subcircuit (R_2Q_2) is assigned to the OER and the R_2 represent the charge transfer resistance (R_{ct}). This parameter decreased exponentially, for all investigated oxides, when the applied potential increased.

The interface capacitance C_{dl} values, given in Tables 1 to 3, were computed using the following relation [24, 25]:

$$Q_2 = (C_{dl})^n * [(R_s)^{-1} + (R_{ct})^{-1}]^{1-n} \quad (2)$$

The equation (2) was given by Brug et al [24] and used to estimate the C_{dl} when the CPE is coupled with the charge transfer resistance.

Values of the apparent current density (i) at different potentials in the OER region (i.e., at $E \geq 0.50$ V) were estimated using the relation (3) [16],

$$R_{ct} = RT / nFi \quad (3)$$

Table 1. Estimates of the circuit parameters for the Co_3O_4 electrodes in 1 M KOH at high anodic potential

E (V vs. SCE)	$10^5 \chi^2$	$10^6 L$ (H cm^2)	R_s ($\Omega \text{ cm}^2$)	$10^4 Q_1$ ($\text{S s}^n \text{ cm}^{-2}$)	n_1	$10^5 \tau_1$ (s)	R_1 ($\Omega \text{ cm}^2$)
0.00	9.9	3.63	2.7	13.95	0.39	3.4	13.0
0.10	6.0	3.20	3.4	13.68	0.42	4.7	11.0
0.20	8.1	3.09	3.4	14.32	0.42	4.4	10.3
0.30	12.5	3.41	2.6	24.00	0.37	5.0	10.7
0.50	9.9	2.85	3.2	40.17	0.37	0.1	8.7
0.60	8.7	2.60	3.9	34.33	0.44	0.2	7.5
0.70	9.6	2.57	4.2	43.00	0.42	30	7.4

E (V vs. SCE)	$10^3 Q_2$ ($\text{S s}^n \text{ cm}^{-2}$)	n_2	τ_2 (s)	R_2 ($\Omega \text{ cm}^2$)	$10^3 C$ (F cm^{-2})	$10^6 Q_2/60$	$10^6 i$ (A cm^{-2})
0.00	5.41	0.83	34.66	3506	2.28	90	
0.10	6.70	0.81	65.10	4392	2.76	112	
0.20	8.21	0.81	22.53	1518	3.53	137	
0.30	8.85	0.88	66.90	4565	5.29	148	
0.50	22.70	0.88	1.01	128.9	15.82		50
0.60	30.90	0.86	0.06	3.6	19.43		1780
0.70	40.90	1.00	0.03	0.80	40.90		8011

Where R , T , n , F and i are the molar gas constant ($\text{J mol}^{-1}\text{K}^{-1}$), temperature (K), number of electrons involved in the reaction, which is 4 in the present case, Faraday constant and the apparent current density (A cm^{-2}), respectively. The apparent current density values, thus estimated, were found to be 50, 4.5 and $0.36 \times 10^{-6} \text{ A cm}^{-2}$ at $E = 0.5$ V, for 0, 5 and 10 % Fe respectively. From these values it can be concluded that the introduction of small amounts of Fe in the Co_3O_4 spinel lattice leads to a decrease on the apparent activity for the OER. This conclusion is in accordance with our previous results obtained by Tafel analysis [10].

Moreover, the equation (2) used to estimate the Cdl gives a good value when the CPE is coupled with the charge transfer resistance, i.e., in the oxygen evolution region. Before O_2 evolution, the interface behaves more or less capacitance like and there is little evidence for the charge transfer resistance. So, the estimated C_{dl} using the relation (2) may not be reliable. Further, results shown in Tables 1-3 show that the values of n_2 are closed to 1 which implies $Q_2 \approx C_2$. Therefore the roughness factor values (R_F), given in the Tables, have been calculated at lower potentials based on the double layer capacitance of a smooth oxide surface ($60 \mu\text{F cm}^{-2}$) [26] using the relation $R_F = Q_2 / 60$. The values found, between 0 and 0.10 V, are 101 ± 10 , 72 ± 11 and 90 ± 4 . As it can be seen, the lower roughness factor was obtained for the oxide samples containing Fe. From these values it can be

concluded that the introduction of small amount of Fe on the oxide composition leads to coatings with a lower surface roughness. This result is in good agreement with the values previously obtained by us for the same oxides at $E = 0$ V vs. SCE using the cyclic voltammetry (59 ± 3 , 47 ± 2 and 48 ± 3) and EIS (79, ~ 54 and ~ 58) for the oxides with 0, 5 and 10% Fe respectively [10]. Thus, the total capacitance reaches its highest value for the Co_3O_4 film.

Table 2. Estimates of the circuit parameters for the Fe- Co_3O_4 5% electrodes in 1 M KOH at high anodic potential

E (V vs. SCE)	$10^4 \chi^2$	$10^6 L$ (H cm^2)	R_s ($\Omega \text{ cm}^2$)	$10^3 Q_1$ ($\text{S s}^n \text{ cm}^2$)	n_1	$10^3 \tau_1$ (s)	R_1 ($\Omega \text{ cm}^2$)
0.0	11	2.56	1.9	0.85	0.66	0.51	8.12
0.1	6.37	2.03	1.5	1.94	0.59	0.38	4.87
0.2	5.05	1.87	1.5	2.26	0.60	0.44	4.08
0.3	4.27	1.94	1.5	2.84	0.59	3.90	4.19
0.4	3.63	1.92	1.5	2.71	0.61	0.52	3.72
0.5	2.65	2.12	1.4	7.30	0.53	9	3.37
0.8	0.34	1.87	1.5	0.34	0.88	0.11	0.94

E (V vs. SCE)	$10^3 Q_2$ ($\text{S s}^n \text{ cm}^2$)	n_2	τ_2 (s)	R_2 ($\Omega \text{ cm}^2$)	$10^3 C$ (F cm^2)	$10^6 Q_2/60$	$10^6 i$ (A cm^2)
0.0	3.83	0.87	-	1×10^{20}	$\sim 3.83^*$	64	
0.1	4.81	0.89	117.3	14440	$\sim 4.81^*$	80	
0.2	7.40	0.84	15.3	1353	3.14	123	
0.3	8.35	0.90	58.9	4690	5.13	139	
0.4	21.41	0.87	323.1	7157	12.80		
0.5	26.49	0.89	4.4	141.8	17.60		4.5
0.8	68.25	0.79	$8.21 \text{ e-}3$	0.33	23.60		19438

4. CONCLUSIONS

This work was undertaken to elucidate the electrochemical behaviour of Fe- Co_3O_4 oxide thin film anodes for the oxygen evolution reaction in 1M KOH, using CV and EIS techniques. The electrical equivalent circuit, L (R_1Q_1) (R_2Q_2) was used in the potential region between the open circuit and oxygen evolution. At each selected potential, a good correlation between experimental and simulated data is found, thereby validating the proposed equivalent circuit model.

The apparent activity toward oxygen evolution reaction and the roughness factor decreased with the presence of Fe in the oxide matrix.

These results are in good agreement with those previously obtained by us using other techniques.

Table 3. Estimates of the circuit parameters for the Fe- Co₃O₄ 10% electrodes in 1 M KOH at high anodic potential

E (V vs. SCE)	$10^5 \chi^2$	$10^5 L$ (H cm ²)	R_s (Ω cm ²)	$10^3 Q_1$ (S s ⁿ cm ²)	n_1	$10^3 \tau_1$ (s)	R_1 (Ω cm ²)
0.0	0.28	22.60	2.1	0.53	0.70	0.58	10.3
0.1	2.49	13.20	13.0	8.20	0.42	1.32	7.5
0.2	2.48	-	12.3	7.08	0.45	0.91	6.0
0.3	5.98	-	11.7	14.62	0.35	2.42	8.3
0.4	5.70	-	10.5	18.96	0.31	2.28	8.0
0.5	4.62	0.03	8.3	34.20	0.29	5.61	6.5
0.6	4.62	0.09	6.5	15.11	0.43	1.00	3.4
0.8	3.85	0.23	4.0	2.40	0.64	0.17	1.6

E (V vs. SCE)	$10^3 Q_2$ (S s ⁿ cm ²)	n_2	τ_2 (s)	R_2 (Ω cm ²)	$10^3 C$ (F cm ²)	$10^6 Q_2/60$	$10^6 i$ (A cm ⁻²)
0.0	5.3	0.81	-	50530	1.85	88	
0.1	5.5	0.90	59.79	7221	4.10	92	
0.2	8.0	0.84	21.67	1656	5.14	133	
0.3	8.3	0.92	24.64	2297	6.77	138	
0.4	18.1	0.92	42.59	1743	15.66		
0.5	27.9	0.93	5.85	185.3	24.91		036
0.6	46.0	0.89	0.11	2.9	34.30		2180
0.8	63.1	0.88	0.02	0.5	38.79		12812

L, R_s, R₁ R₂, Q₁, Q₂ stand for inductance, solution resistance, resistance of the oxide film, charge transfer resistance, constant phase element, double layer capacitance, respectively

ACKNOWLEDGEMENTS

The authors gratefully acknowledge the support of this work by CNRST (Maroc) and GRICES (Portugal) under Research Convention project.

References

1. S. Trasatti, G. Lodi in: S. Trasatti (ed) Electrodes of conductive mettalic oxides, Part B. Elsevier, Amsterdam (1980),p. 521 and references therein
2. M.R. Tarasevich, B.M. Efremov in: Trasatti S (ed) Electrodes of conductive mettalic oxides, Part B. Elsevier, Amsterdam (1980), p. 221 and references therein
3. S.Trasatti in: J. Lipkowski, P.N. Ross (ed) Electrochemistry of novel materials. VCH publishers Inc, New York. (1994), p. 207 and references therein
4. M. Hamdani, M.I.S. Pereira, J. Douch, A. Ait Addi , Y. Berghoute, M.H. Mendonça Electrochim Acta, 49 (2004) 1555
5. R.N. Singh, M. Hamdani, J.F. Koenig, P. Chartier, *J. Appl. Electrochem.* 20 (1990) 442
6. R.N. Singh, J.F. Koenig, G. Poillerat, P. Chartier, *J. Electrochem. Soc.*, 137 (1990) 1408
7. Y. Qi, Y. Zhao, Z .Wu, *Mater. Chem. Phys.*, 110 (2008) 457
8. S.Y. Lian, E.B. Wang , L.Gao, L. Xu, *Mater. Lett.*, 61 (2007) 2894

9. Y. Dian, P. Zhang, Z. Long, Y. Jiang, J. Huang, W. Yan, G. Liu, *Mater. Lett.*, 62 (2008) 3410
10. E. Laouini, M. Hamdani, M.I.S. Pereira, J. Douch, M. H.Mendonça, Y. Berghoute, R.N. Singh, *Int. J. Hydrogen Energy*, 33 (2008) 4936
11. E. Laouini, M. Hamdani, M.I.S. Pereira, J. Douch, M. H.Mendonça, Y. Berghoute, R.N. Singh, *J. Appl. Electrochem.*, 38 (2008) 1485
12. N. Priyantha, P. Jayaweera, D.D. Macdonalt, A. Sun, *J. Electroanal. Chem.*, 572 (2004) 409
13. C. Clerc, R..C. Alkire in: W.H. Smyrl, Proceeding of the symposium on Transient Techniques in corrosion Science and Engineering, Proceeding D.D. Macdonald (ed) (1989), Volume 89-1 P.57
14. V.A. Alves, L. A. Da Silva., J.F.C. Boodts, *Electrochim. Acta*, 44 (1998) 1525
15. E.B. Castro, S.G. Real, L.F. Pinheiro Dick, *Int. J. Hydrogen. Energy*, 29 (2004) 255
16. S. Palmas, F. Ferrara, A. Vacca, M. Mascia, A.M. Polcaro, *Electrochim. Acta*, 53 (2007) 400
17. D.T. Shieh, B.J. Hwang, *Electrochim. Acta*, 38 (1993) 2239
18. G.C. Silva, C.S. Fugivara, G. Tremiliosi Filho, P.T.A. Sumodjo, A.V. Benedetti, *Electrochim. Acta*, 47 (2002) 1875
19. R.N. Singh, D. Mishra, Anindita, A.S.K. Sinha, A. Singh, *Electrochem. Comm.*, 9 (2007) 1369
20. J.O'M Bockris, A.K.N Reddy, M. Gamboa-Aldeco in: "Modern Electrochemistry Vol. 2A, 2nd Edition", Kluwer Academic/Plenum Publishers, New York, (2000) p. 1132
21. R.N. Singh, M. Malviya, Anindita, A.S.K. Sinha, P. Chartier, *Electrochim. Acta*, 52 (2007) 4264
22. N.K. Singh, S.K. Tiwari, K.L. Anitha, R.N. Singh, *J. Chem. Soc. Faraday Trans.*, 92 (1996) 2397
23. R.N. Singh, N.K. Singh, J.P. Singh, G. Balaji, N.S Gajbhiye, *Int. J. Hydrogen Energy*, 31 (2006) 701
24. G.J. Brug, A.L.G. van den Eeden, M.S. Rehbach, J.H. Sluters, *J. Electroanal. Chem.*, 176 (1984) 275
25. R.N. Singh, T. Sharma, A. Singh, Anindita, D. Mishra, S.K. Tiwari, *Electrochim. Acta*, 53 (2008) 2322
26. S. Levine, A. L. Smith, *Discuss. Faraday Soc.*, 52 (1971) 290